

Raman spectroscopy of $\text{Co}(\text{OH})_2$ at high pressures: Implications for amorphization and hydrogen repulsion

Sean R. Shieh* and Thomas S. Duffy

Department of Geosciences, Princeton University, Princeton, New Jersey 08544

(Received 13 September 2001; published 30 October 2002)

Raman spectra of cobalt hydroxide $\text{Co}(\text{OH})_2$ were recorded to 31 GPa using a diamond anvil cell. In contrast to a previous infrared (IR) spectroscopic study, our Raman data show no sharp change in the O-H stretch peak width near 11 GPa, ruling out the possibility of abrupt hydrogen sublattice amorphization at this pressure. This is consistent with neutron diffraction data for $\text{Co}(\text{OD})_2$ to 16 GPa which shows no evidence for such amorphization but instead indicates a possible change in local D ordering in response to $D \cdots D$ repulsion. However, in agreement with the IR work, we find that the peak width of the OH stretch mode increases significantly over a broad pressure interval from 10 to 25 GPa and reaches $\sim 200 \text{ cm}^{-1}$ at 25 GPa. An energy dispersive x-ray diffraction study carried out to 48 GPa indicates that $\text{Co}(\text{OH})_2$ remains crystalline to at least this pressure, although evidence for some anomalous broadening of x-ray peaks is observed at ~ 26 GPa. The peak widths ($> 200 \text{ cm}^{-1}$) of both the Raman and infrared stretching vibration of $\text{Co}(\text{OH})_2$ are indicative of a high degree of disorder of the H positions while only minimal disordering of the Co-O substructure is allowed by the x-ray data. Thus, the possibility of substructure amorphization remains viable, but through a process of continuous disordering over a broad pressure interval rather than as a discrete discontinuity. Repulsion between neighboring H atoms is likely to be an important driving force for this disordering as suggested by previous neutron and theoretical studies, but it remains uncertain whether such a model can quantitatively describe the range of observed peak widths at high pressures.

DOI: 10.1103/PhysRevB.66.134301

PACS number(s): 62.50.+p, 63.20.-e, 33.20.Fb, 33.20.Tp

INTRODUCTION

The high-pressure behavior of brucite-type hydroxides has been extensively examined in recent years as a model system for understanding hydrogen-bearing materials under compression. Studies have revealed a complex and varied range of phenomena in these apparently simple materials, including pressure-induced amorphization,¹⁻⁴ sublattice (H-layer) amorphization,⁵ crystal structure changes,⁶ shifts in hydrogen positions,^{7,8} hydrogen repulsion,^{9,10} and structural frustration.¹¹ The role of hydrogen bonding in these materials has also been controversial.^{1,4,11-13} Cobalt hydroxide $\text{Co}(\text{OH})_2$ is isostructural with $\text{Mg}(\text{OH})_2$ and $\text{Ca}(\text{OH})_2$ and crystallizes in the CdI_2 structure ($P\bar{3}m1$, $Z=1$) at ambient conditions¹⁴ [Fig. 1(a)]. The hydrogen atoms are isolated between layers of MO_6 octahedra where M is a divalent cation such as Fe, Co, Ni, Cd, Mg, or Ca. The MO_6 octahedra are compressed along the c axis creating a distorted hexagonal close packing of oxygens. Each oxygen is hydrogenated and in the ideal structure the O-H groups lie along the threefold symmetry axis and are equidistant from the three oppositely orientated O-H groups in the neighboring layer below each hydroxyl unit [Fig. 1(b)]. Neutron diffraction studies have reported unusual thermal motion for the H atom.^{14,15} More recently an alternate model for these materials has been proposed whereby the H atom is split over three sites making an angle of $\sim 10^\circ$ with respect to the c axis.^{10,13,16,17} X-ray and neutron diffraction data^{5,9} show that the c axis is initially much more compressible than the a axis. This is a general feature of the compression of brucite-type hydroxides.^{1,2,8,13,14,18} Compression will therefore enhance the interaction of $\text{O} \cdots \text{H}$ and $\text{H} \cdots \text{H}$ units between neighboring layers.

X-ray diffraction studies on $\text{Ca}(\text{OH})_2$ (portlandite) reported conclusive evidence for complete amorphization at pressures near 12 GPa from the combined observations of sudden loss of x-ray diffraction peak intensity and the pronounced broadening of the O-H stretching vibration.^{1,2} On the other hand, brucite [$\text{Mg}(\text{OH})_2$] was found to remain

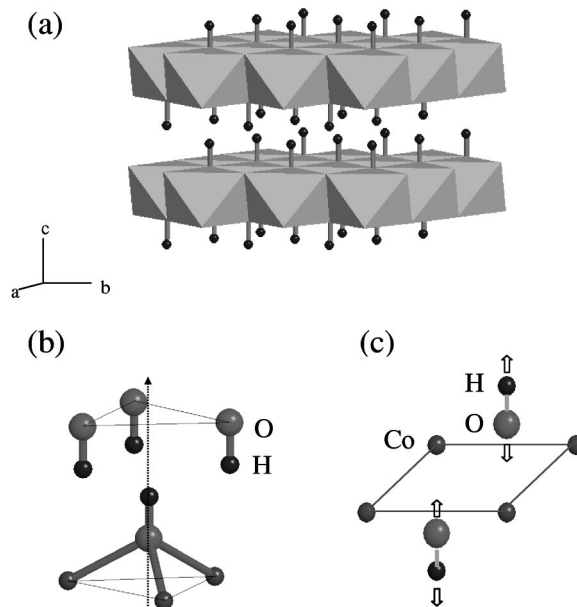


FIG. 1. Crystal structure of $\text{Co}(\text{OH})_2$. (a) $(\text{MO})_6$ octahedral layers with H atoms shown as spheres. (b) Local H environment showing the antiferromagnetic arrangement of oppositely oriented OH groups (after Ref. 11) (c) Raman-active symmetric O-H stretching vibration.

crystalline to pressures above 30 GPa from x-ray, infrared, and Raman studies.^{1,3,7,8,14}

Using infrared, Raman, and x-ray data, Nguyen *et al.*⁵ reported a novel form of sublattice (H layer) amorphization occurring in $\text{Co}(\text{OH})_2$ at about 11.2 GPa. Their evidence consisted of a pronounced broadening of the IR O-H (out-of-phase) stretching mode and a loss of intensity of Raman peaks [in-phase stretching mode, Fig. 1(c)] over a narrow pressure range, but no accompanying change in the x-ray diffraction pattern. Evidence for precursory disordering of the H sublattice in $\text{Ca}(\text{OH})_2$ has also been reported in a Raman study.³

However, recent neutron diffraction studies of $\text{Co}(\text{OD})_2$ by Parise and colleagues¹⁰ revealed no evidence for abrupt amorphization of the hydrogen sublattice. The minor differences in behavior between D and H atoms are considered to be negligible in this regard. The D-site occupancy was found to remain constant through the spectroscopic discontinuity up to the maximum pressure studied of 16 GPa. The neutron diffraction studies show that the effect of pressure is to shift the D atoms off the three-fold site $2d$ at $(1/3, 2/3, z)$ to 3 equivalent sites $6i$ at $(x, 2x, z)$ with occupation factor $1/3$ for both $\text{Mg}(\text{OD})_2$ (Ref. 7) and $\text{Co}(\text{OD})_2$,⁹ consistent with low-temperature neutron data for alkaline earth hydroxides.^{16,17} Parise's^{10,13} model further suggests that when the pressure reaches near 11 GPa for $\text{Co}(\text{OD})_2$, the effects of interlayer compression together with displacement of the H(D) atoms lead to a violation of empirical constraints on minimum allowed H(D) \cdots H(D) distances. The resulting H(D) \cdots H(D) repulsion drives the H(D) atoms from the $6i$ sites to a range of positions on circles of constant displacement from the threefold axis. The final arrangement of atoms is a spatial and temporal mixture of H environments described as a highly disordered (but crystalline) proton arrangement and the spectroscopic anomaly is attributed to a hydrogen repulsion "transition."¹⁰

This problem has also been addressed by a recent *ab initio* molecular dynamics simulation carried out for both $\text{Ca}(\text{OH})_2$ and $\text{Mg}(\text{OH})_2$ up to 14 GPa.¹¹ The simulation results are consistent with the neutron studies in that the H atoms are found to move to $6i$ sites (with $1/3$ occupancy) for both $\text{Ca}(\text{OH})_2$ and $\text{Mg}(\text{OH})_2$ at high pressures. This ultimately leads to a loss of long-range order among the H positions, as formation of an ordered array is prevented by H repulsion and the topology of the lattice. This produces a strong broadening of the IR stretch vibration in $\text{Ca}(\text{OH})_2$ but the effect is less pronounced in $\text{Mg}(\text{OH})_2$. Interestingly, the amorphization of the Ca-O substructure is not addressed in this study. This means that strong broadening of the IR mode by this mechanism can be decoupled from M-O sublattice amorphization which is exactly what is observed for $\text{Co}(\text{OH})_2$. However, the lack of broadening found for $\text{Mg}(\text{OH})_2$ is attributed to the smaller size of the Mg^{2+} cation relative to Ca^{2+} (resulting in more limited atomic displacements and hence sharper IR bands). Since Co^{2+} (0.77 \AA) is similar in size to Mg^{2+} (0.72 \AA) and both are much smaller than Ca^{2+} (1.00 \AA), it is thus questionable whether this mechanism can reproduce the magnitude of the extreme IR broadening observed in $\text{Co}(\text{OH})_2$ unless other effects are important. Fur-

thermore, the sudden onset of the spectroscopic anomaly is not explained by these models. In order to further explore the nature of the high-pressure state in this transition metal hydroxide, we have performed Raman spectroscopy and x-ray diffraction on $\text{Co}(\text{OH})_2$ to pressures well above the proposed IR anomaly.

EXPERIMENTS

The starting material (Alfa Aesar, 99.9%) was confirmed to be pure $\beta\text{-Co}(\text{OH})_2$ by x-ray diffraction at ambient pressure. The sample was loaded into a steel gasket hole ($30\text{-}\mu\text{m}$ thick and $150\text{-}\mu\text{m}$ diameter) of a symmetric diamond anvil cell with $300\text{-}\mu\text{m}$ culets. Also loaded were $\sim 1\text{-}\mu\text{m}$ ruby chips and argon to serve as a pressure-transmitting medium. Pressure was determined by the ruby fluorescence method.¹⁹ An argon ion laser (514.5 nm) served as the excitation source. In order to prevent chemical reactions or dehydration during the experiments, the laser output power was controlled to less than 50 mW. The micro-Raman system used here consists of holographic optics, a single (1800 groove/mm) grating, 0.5-m spectrometer, and a liquid nitrogen cooled CCD detector ($1100 \times 330 \text{ pixels}$).^{20,21} The spectrometer was regularly calibrated using the neon emission spectrum. The precision of the measured frequency is better than $\pm 2 \text{ cm}^{-1}$. Experiments were performed using low-fluorescence diamond anvils and a 135° scattering geometry. Typical collection times in the lattice mode and O-H vibrational regions were 15 and 30 mins, respectively, with three total accumulations. The Raman data were fitted to a combination of Lorentzian and Gaussian modes. The Raman spectrum of our starting material showed four lattice modes (250 , 427 , 503 , and 547 cm^{-1}) and one OH vibrational mode (3572 cm^{-1}) (Fig. 2).

Group theory analysis of the zone-center phonon modes of brucite-type hydroxides demonstrate that the total irreducible representation is $\Gamma = 2A_{1g} + 3A_{2u} + 2E_g + 3E_u$.^{22,23} Four Raman active modes are allowed, three of which are lattice modes and one is a symmetric OH stretching vibration. By comparison with ambient-pressure data on other brucite-type hydroxides (Table I), the lowest-frequency lattice modes (250 and 427 cm^{-1}) can be assigned as $E_g(T)$ and $A_{1g}(T)$, respectively. In alkaline earth hydroxides, the $E_g(R)$ mode is weak and occurs near 700 cm^{-1} . Thus, the assignment of the modes at 503 and 547 cm^{-1} is unclear, although it is possible that one of these is the $E_g(R)$ mode. Extra Raman peaks in the lattice vibration region have also been reported for $\text{Ni}(\text{OH})_2$ and attributed to structural defects, proton vacancies, and chemical impurities.^{24,25} The mode at 503 cm^{-1} lies close to the frequency of the $A_{2u}(T)$ infrared active mode (510 or 522 cm^{-1})^{23,26} (Table I) and hence we tentatively make this assignment. However, it should be noted that the assignments of the $A_{2u}(T)$ and $E_u(R)$ modes is presently uncertain.^{23,26} In $\text{Mg}(\text{OH})_2$, an extra lattice mode was also observed at high pressures and when extrapolated to 1 bar was found to occur at a similar frequency to the $E_u(R)$ infrared active mode.⁶ The mode at 547 cm^{-1} has the weak, broad character typically found for hydroxide rotational modes and we tentatively assign this to

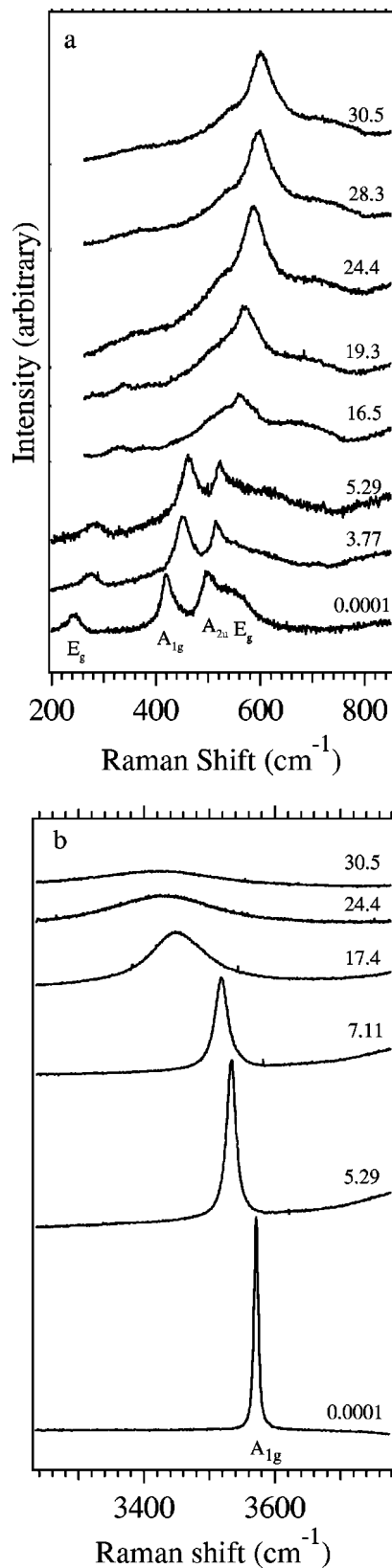


FIG. 2. Representative Raman spectra of $\text{Co}(\text{OH})_2$ to 31 GPa in (a) external mode region and (b) internal (OH-stretching) mode region. The peak assignment is shown for each mode and pressure (in GPa) is indicated on the right-hand side of each spectrum.

be the $E_g(R)$ mode. All Raman and infrared translational lattice mode vibrational frequencies for transition metal hydroxides decrease as a function of increasing M -O bond distance as observed previously for the O-H infrared stretching frequency.^{23,27} The assignments we have made here are fully consistent with this progression (Table I).

For x-ray diffraction experiments, the starting material was from the same source as used in the Raman measurements. The $\text{Co}(\text{OH})_2$ sample together with a 30- μm diameter Au foil and ruby chips were loaded together with an argon pressure-transmitting medium in a stainless steel gasket in a diamond-anvil cell with 300- μm culets. Pressure was determined from both ruby fluorescence and the equation of state of Au.²⁸ X-ray diffraction patterns were collected at beamline X17C, National Synchrotron Light Source using energy-dispersive techniques ($8 \times 16 \mu\text{m}$ beamsize) and a solid state detector. The diffraction angle was calibrated using a gold foil, and the detector was calibrated with a series of fluorescence standards.

RESULTS

For Raman measurements, $\text{Co}(\text{OH})_2$ was pressurized to a maximum of 31 GPa and spectra were recorded upon both compression and decompression (Figs. 2 and 3). All lattice modes increase with compression and were observed to persist to the highest pressure, although most exhibit considerable broadening (Fig. 2). Upon decompression, the behavior of the lattice modes was largely reversible with little hysteresis, although irreversible changes in the relative peak intensities were observed upon decompression back to ambient pressure. The intensity of the $A_{1g}(T)$ mode decreased strongly with compression, and this mode has a markedly nonlinear pressure dependence. The $A_{2u}(T)$ mode became the dominant feature of the spectrum at pressures above 16 GPa, which is surprising since this mode is formally Raman inactive. If our assignment of the $A_{2u}(T)$ mode is correct, then the relative behavior of this mode and the $A_{1g}(T)$ could be explained by a weak Fermi resonance. Such a resonance occurs as a result of anharmonic coupling of two nearly degenerate vibrational modes of the same character. A Fermi resonance between the $E_g(T)$ mode and what was identified as a probable $E_u(T)$ mode was documented in $\text{Mg}(\text{OH})_2$.⁶ For $\text{Co}(\text{OH})_2$, the intensity shift and frequency separation are consistent with a resonant interaction, although the closest approach of the two modes is only about 50 cm^{-1} in this case, compared with 18 cm^{-1} for $\text{Mg}(\text{OH})_2$.

The A_{1g} O-H internal mode weakened and broadened with pressure [Fig. 2(b)] but reverted without hysteresis upon decompression. This reversibility is in good agreement with observations from IR and Raman on $\text{Co}(\text{OH})_2$ (Refs. 4,5) and $\text{Mg}(\text{OH})_2$.^{1,6} The OH stretching vibration has a negative pressure dependence whose slope is given by $dv/dP = -9.60 + 0.15P \text{ cm}^{-1}/\text{GPa}$. This initial slope is greater than that observed for the alkaline earth hydroxides $\text{Mg}(\text{OH})_2$ (Ref. 3) and $\text{Ca}(\text{OH})_2$,³ as well as $\text{Ni}(\text{OH})_2$ (Ref. 29) (Fig. 4). In contrast to the other materials, however, the rate of decrease weakens above 15 GPa and the OH-stretch frequency becomes nearly pressure independent above 25 GPa.

TABLE I. Raman and infrared vibrational modes (in cm^{-1}) and M -O distances in brucite-type hydroxides.

Compound	Stretching mode		Librations R		Lattice vibrations T				M -O(\AA)	Ref.
	A_{1g}	A_{2u}	E_g	E_u	A_{1g}	A_{2u}	E_g	E_u		
$\text{Mg}(\text{OH})_2$	3652	3688	725	415	443	455	280	361	2.099	36
	3652.0		727.5		444.7		280.0			6
	3661.3									6
$\text{Ca}(\text{OH})_2$	3620	3640	680	373	357	334	254	288	2.369	36
$\text{Mn}(\text{OH})_2$	3578	3625		386	401	432	234	283	2.186	23
$\text{Fe}(\text{OH})_2$	3576	3624		395	407	488	260	305	2.139	23
β - $\text{Co}(\text{OH})_2$	3559	3630		433		510		314	2.115	23
	3572		547?		427	503?	250			This study
β - $\text{Ni}(\text{OH})_2$	3580	3639		452	449	530	318	350	2.073	23
	3580				446		312			29,37
β - $\text{Cd}(\text{OH})_2$	3566	3607		330	382	435	232	255	2.314	23

A similar flattening in the pressure dependence of the OH-stretch frequency is observed in the IR data at lower pressures.⁴ However, it is difficult to accurately obtain peak centroids for these broad, low-amplitude peaks [Fig. 2(b)].

The pressure dependence of the Raman frequency for $\text{Co}(\text{OH})_2$ observed here closely tracks that reported for a low-frequency shoulder on the IR stretch vibration.⁴ In the IR work, this shoulder, which was detectable to 20 GPa, was identified as a hot band caused by the transition from the first excited state to the first overtone.⁴ Our results suggest that this shoulder might instead be the Raman-active symmetric stretch vibration. Similar features have been identified in both Raman and IR spectra for brucite^{1,6,30} and interpreted as a mixing of formally infrared and Raman modes due to structural distortion or disorder.

The full width at half maximum (FWHM) of the O-H stretching peak shows a continuous increase with pressure

(Fig. 5). This is inconsistent with the earlier spectroscopic study^{4,5} which reported a sudden loss of Raman intensity and broadening of the IR peak width for the O-H vibrational modes at 11.2 GPa. The difference in the Raman behavior can be explained by the higher quality signal obtained in this study using an improved micro-Raman spectrometer. Our dense distribution of data points upon both increasing and decreasing pressure rules out the existence of a sharp spectroscopic anomaly. Figure 6 shows the continuous variation of peak width in the critical region between 9 and 17 GPa. Other features of the present data, however, are consistent with the IR measurements. First, we observe that the rate of broadening is larger in the 10-25 GPa pressure interval than above or below this range. Below 10 GPa, the FWHM has a curvative similar to that reported for $\text{Mg}(\text{OH})_2$. Above 25 GPa, the peak width curve flattens consistent with IR data at

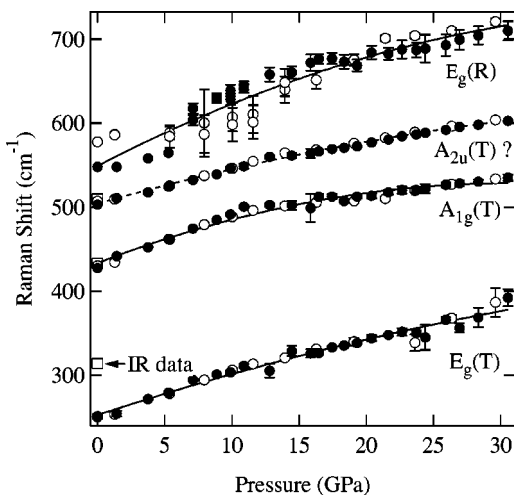


FIG. 3. Pressure-induced frequency shifts of external phonon modes. Solid circles indicate data measured during compression and open symbols are data measured during decompression. Solid and dashed lines are polynomial fits to the data. Error bars are smaller than the symbol size when not shown. The open squares show ambient pressure infrared data (Ref. 23).

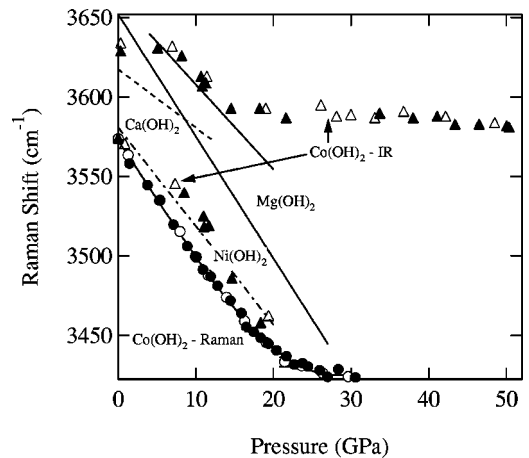


FIG. 4. Raman shift of the OH vibrational mode of $\text{Co}(\text{OH})_2$ as a function of pressure. The solid and dashed lines are fits to data for $\text{Mg}(\text{OH})_2$, $\text{Ca}(\text{OH})_2$, respectively (Refs. 2,3,18). The dash-dotted line is a fit to the data of Ref. 29. The solid and open triangles are infrared data from Nguyen *et al.* (Ref. 4). The solid and open circles are Raman data obtained in this study. All solid symbols represent compression data and open ones represent decompression data.

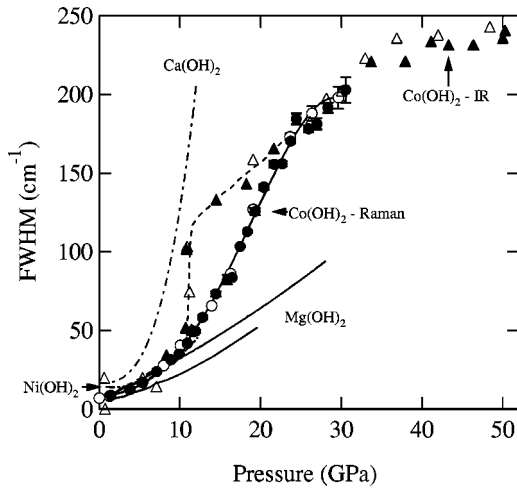


FIG. 5. Full width at half maximum (FWHM) of the OH vibrational peak of $\text{Co}(\text{OH})_2$ as a function of pressure. The circles are Raman data from this study and the triangles show the antisymmetric infrared fundamental vibration (Refs. 4,5) (the dashed curve shows a fit to this data). All solid symbols are compression data and open symbols are decompression data. The dash-dotted, solid, and dashed curves are fits to data for $\text{Ca}(\text{OH})_2$, $\text{Mg}(\text{OH})_2$, and $\text{Ni}(\text{OH})_2$, respectively (Refs. 2,3,18,29). Upper and lower curves for $\text{Mg}(\text{OH})_2$ are data taken under non-hydrostatic and quasihydrostatic conditions, respectively.

higher pressures. Compared with $\text{Mg}(\text{OH})_2$ the broader peak widths in $\text{Co}(\text{OH})_2$ indicate the H atoms are in a much more disordered state. By 25 GPa, the peak widths in $\text{Co}(\text{OH})_2$ are comparable to those in $\text{Ca}(\text{OH})_2$ in the region of pressure-induced amorphization.

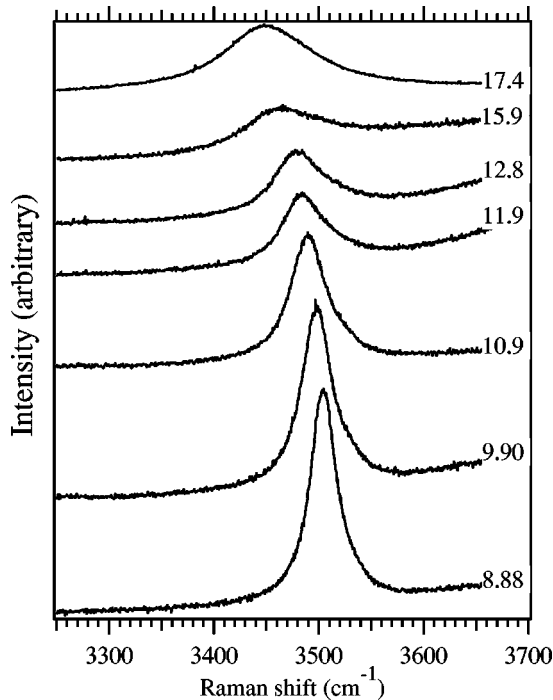


FIG. 6. OH stretching vibration in $\text{Co}(\text{OH})_2$ between 9 and 17 GPa.

TABLE II. (a) The pressure-dependence of the vibrational modes obtained from polynomial fits and the mode Grüneisen parameters of $\text{Co}(\text{OH})_2$. (b) Comparison of zero-pressure mode Grüneisen parameters for brucite-type hydroxides.

ν_0 (cm^{-1})	$\partial\nu/\partial P$ ($\text{cm}^{-1}/\text{GPa}$)	$\partial^2\nu/\partial P^2$ ($\text{cm}^{-1}/\text{GPa}^2$)	γ_{i0}
250	5.232	-0.037	1.009
427	6.161	-0.0998	0.692
503	4.531	-0.0422	0.438
547	8.300	-0.0921	0.736
3572	-9.601	0.1457	-0.131

Mode	(b)		
	$\text{Co}(\text{OH})_2$ γ_{i0}	$\text{Mg}(\text{OH})_2^a$ γ_{i0}	$\text{Ca}(\text{OH})_2^a$ γ_{i0}
$E_g(T)$	1.01	0.81	0.85
$A_{1g}(T)$	0.69	0.65	0.94
$E_g(R)$	0.74		1.21
$A_{1g}(I)$	-0.13	-0.09	-0.04

^aData from Ref. 3.

The mode-Grüneisen parameter (γ_i) can be expressed by the volume dependence of the frequency for the i th vibration mode (ν_i) in the crystal

$$\gamma_i = -[(d \ln \nu_i)/(d \ln V)] = (K_T/\nu_i)(d\nu_i/dP),$$

where K_T is the bulk modulus. Using the slope ($d\nu_i/dP$) of each lattice mode from our measurements and the bulk modulus ($K_T=49$ GPa), we calculated the Grüneisen parameter (ν_i) for each mode as a function of pressure (Table II, Fig. 7).

X-ray diffraction patterns show clearly that $\text{Co}(\text{OH})_2$ remains crystalline to 48 GPa (Fig. 8). The decrease in intensity with pressure is typical and can be attributed to sample

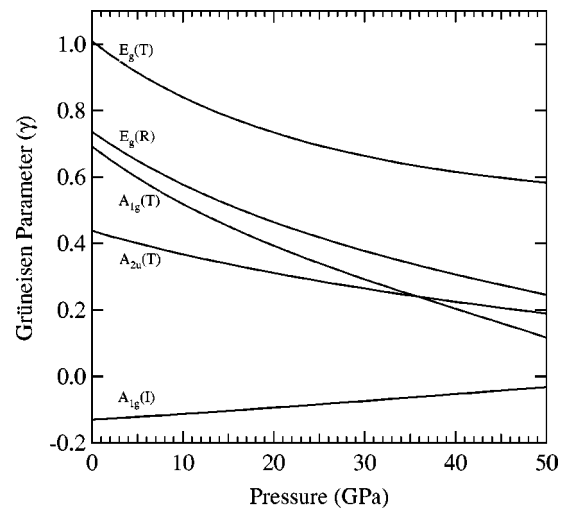


FIG. 7. The mode Grüneisen parameters of $\text{Co}(\text{OH})_2$ as a function of pressure.

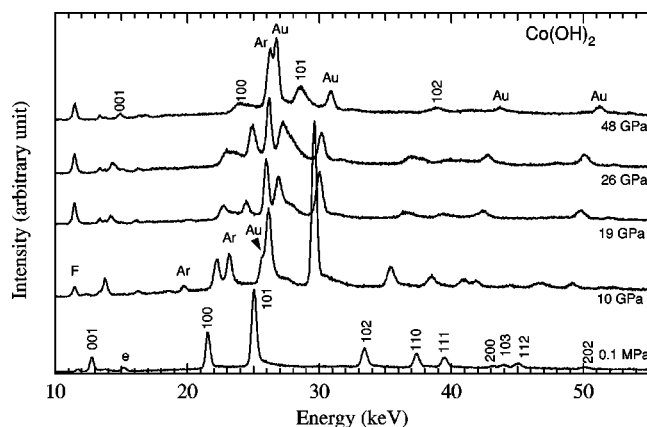


FIG. 8. Selected x-ray diffraction patterns of $\text{Co}(\text{OH})_2$ as a function of pressure. The Miller indices (hkl) denote peaks from $\text{Co}(\text{OH})_2$, while lines from gold and argon are labeled Au and Ar, respectively. F marks the location of fluorescence peaks, while e indicates escape peaks from the Ge detector.

thinning and effects of deviatoric stress. The peak widths increases gradually with pressure below 26 GPa consistent with an increase in deviatoric stress, but broaden markedly relative to Au and Ar peaks at pressure near 26 GPa (Fig. 8). This broadening is greater than expected from the effects of the nonhydrostatic stress field. However, no new or unexplained diffraction peaks are clearly observed. Our results extend earlier studies^{5,9,10} that reported no pressure-induced amorphization of the Co-O substructure to at least 23 GPa. However, our results suggest that $\text{Co}(\text{OH})_2$ is more compressible than found in an earlier study⁵ probably due to the lack of pressure-transmitting medium in that work. The x-ray diffraction results will be described in more detail in a forthcoming publication.

DISCUSSION

The hypothesis of sublattice amorphization is based upon the loss of Raman signal, abrupt jump of the FWHM of the O-H stretching vibration, and flattening of c/a in x-ray measurements near 11 GPa.⁵ In this study, we find from Raman spectroscopy that both the lattice and OH stretching modes are readily detectable to at least 30 GPa. Furthermore, we find no evidence for an abrupt jump in the FWHM of the Raman active OH stretch vibration, nor do we observe any discontinuity in the variation of OH stretch frequency with pressure as reported by Nguyen *et al.*⁴ Flattening of the c/a ratio with pressure is observed to some degree in all high-pressure hydroxides regardless of whether they undergo amorphization or not.¹³ In combination with the lack of any evidence of an abrupt discontinuity from neutron data,¹⁰ the hypothesis of sublattice amorphization in $\text{Co}(\text{OH})_2$ near 11 GPa can be ruled out. There are, however, important aspects of the vibrational spectra that are consistent between the Raman and IR work, in particular, the extremely broad OH peak width and frequency independence of the OH stretch vibration that are observed above 25 GPa. If the OH stretch frequency is taken to be a proxy for O-H bond length, the pressure dependence of the OH stretch frequency may indi-

cate that the OH bond distance initially decreases with pressure but becomes constant above 25 GPa. However, neutron diffraction studies suggest that O-H and O-D bond lengths do not decrease with pressure despite the redshift of the OH stretch vibrations.¹⁰ These studies do provide strong evidence for the reduction of the H \cdots H distance, however.¹⁰ The frequency redshift of the OH stretch has been observed in studies of other hydroxides and is taken as empirical evidence for hydrogen bonding^{1,4} although this interpretation is disputed by theoretical studies.^{11,12}

At 16 GPa, the highest pressure reached by neutron diffraction, the OH peak width in $\text{Co}(\text{OH})_2$ is about twice as large as in brucite under the same conditions. Figure 5 shows that for brucite the effect of non-hydrostatic stress on the peak width is to cause only modest additional broadening. By 30 GPa, the OH peak width in $\text{Co}(\text{OH})_2$ has increased by an additional factor of 2–3, consistent with the IR observations. Hence, the neutron results at 16 GPa may not be able to provide a clear picture of the structural behavior at higher pressures. That is, disordering of the structure appears to be occurring over a broad pressure interval (10–25 GPa) and the degree of disorder in $\text{Co}(\text{OH})_2$ at 16 GPa is small relative to that at higher pressures.

The peak widths ($>200\text{ cm}^{-1}$) observed for $\text{Co}(\text{OH})_2$ indicate that a broad distribution of O-H bond lengths and bond strengths are present in these samples above 25 GPa. As previously pointed out, the observed peak widths are comparable to those in pressure amorphized $\text{Ca}(\text{OH})_2$, OH, and OD vibrations in liquid water, and hydroxyl peaks in oxide glasses.⁵ In addition, they are also comparable to peak widths observed in infrared spectra of hydrated (Mg,Fe)SiO₃ glasses.³¹ Our FWHM values are also comparable to those observed in the high-pressure hydrous silicate, phase *E* at ambient and high pressure ($\sim 150\text{--}350\text{ cm}^{-1}$) which is known to have cation disorder and is likely to have proton disorder as well.³² Another dense hydrous silicate, phase *D*, has been observed to have a broad ($\sim 300\text{ cm}^{-1}$ FWHM) Raman OH stretching vibration at 1 bar (Ref. 33) as well as structural evidence for H disorder from a single-crystal x-ray diffraction study.³⁴ Broad IR peaks of a few hundred cm^{-1} also characterize other hydrous phases of possible interest in the Earth's mantle, including hydrous ringwoodite.³⁰ Using Libowitzky's³⁵ correlation of OH stretching frequencies and O-H \cdots O bond distance in minerals, the observed peak width would correspond to a range of H \cdots O bond distances from ~ 1.85 to $\sim 2.05\text{ \AA}$.

All these lines of evidence suggest there is a substantial degree of H disorder between the octahedral sheets of $\text{Co}(\text{OH})_2$ developing at pressures between 10 and 25 GPa. It is not clear whether the repulsion-induced local disordering model¹⁰ can explain the magnitude of the disordering observed spectroscopically. Theoretical studies¹¹ of structural frustration resulting from H \cdots H repulsive forces only produce broadening for large cations such as Ca^{2+} and not for small cations such as Mg^{2+} . The larger spacings between OH anions in $\text{Ca}(\text{OH})_2$ allow for a larger range of H displacements compared with $\text{Mg}(\text{OH})_2$. However, the *ab initio* study extended only to 14 GPa, and may not have resulted in sufficient compression for H repulsion effects to manifest

themselves in Mg(OH)₂. In fact, based on both structural data and the empirical value for minimum contact distances for nonbonded H atoms, Parise¹⁰ argues that these repulsion effects will not become important in Mg(OH)₂ until pressures above 30 GPa whereas the effects are expected to manifest themselves around 10 GPa for Co(OH)₂. Future molecular dynamics studies are needed to resolve this issue.

Our results also provide support for Parise's model¹⁰ in that the requirement for a sharp spectroscopic anomaly near 11 GPa is removed. Also, the peaks widths we observe at 16 GPa are only about 50% of those reported in the IR study. This means it is easier to reconcile the the localized H displacements in Parise's model with spectroscopic data at these pressures. Our observations are consistent with a gradual disordering beginning around 10 GPa which is completed by about 25 GPa. This is also more consistent with the proposed driving force for H-layer amorphization in which a continuous reduction of interlayer spacing and hence H···H distance would be expected to promote to a continuous disordering of H positions with pressure. The flattening of the OH peak width beginning above 25 GPa may suggest that a balance between competing forces is ultimately achieved that prevents further disordering. That the x-ray peaks widths change abruptly at a similar pressure suggests that interactions involving the Co-O sublattice may be an important contributor to this balance. The disordering in the H layer may induce a small amount of local disordering in the Co-O layer, but is apparently insufficient to drive the system to complete amorphization.

SUMMARY

Raman spectra and x-ray diffraction patterns have been recorded for Co(OH)₂ to 31 and 48 GPa, respectively. In contrast to previous infrared results but consistent with neutron diffraction studies, no abrupt sublattice (H-layer) amorphization is observed near 11 GPa. However, the OH stretching vibration of Co(OH)₂ markedly broadens over the pressure interval from 10 to 25 GPa and eventually reaches peak widths ($\sim 200\text{--}250\text{cm}^{-1}$) in agreement with IR results and consistent with those observed in a variety of H-disordered materials including pressure-amorphized solids, liquids, hydrous glasses, and hydrous silicates with cation and H disorder. However, x-ray diffraction results to 48 GPa show that the Co-O substructure remains essentially intact although some anomalous broadening is observed near 26 GPa. It is possible to reconcile the IR and neutron results by postulating that H-layer disorder occurs over a broad pressure interval in response to increase hydrogen repulsion as the interlayer distances are reduced.¹⁰ The question of whether this model of localized disorder can reproduce the broad range of O···H distances implied by the spectroscopic data requires further study.

ACKNOWLEDGMENTS

We thank Jingzhu Hu, Alex Goncharov, and Nagayoshi Sata for technical assistance. This work was supported by the NSF and the David and Lucile Packard Foundation.

*Electronic address: shieh@princeton.edu

¹M.B. Kruger, Q. Williams, and R. Jeanloz, *J. Chem. Phys.* **91**, 5910 (1989).

²C. Meade and R. Jeanloz, *Geophys. Res. Lett.* **17**, 1157 (1990).

³T.S. Duffy, R.J. Hemley, and H.K. Mao, in *Volatiles in the Earth and Solar System*, edited by K.A. Farley (American Institute of Physics, Woodbury, NY, 1995), p. 211.

⁴J.H. Nguyen, M.B. Kruger, and R. Jeanloz, *Phys. Rev. B* **49**, 3734 (1994).

⁵J.H. Nguyen, M.B. Kruger, and R. Jeanloz, *Phys. Rev. Lett.* **78**, 1936 (1997).

⁶T.S. Duffy, C. Meade, Y. Fei, H.K. Mao, and R.J. Hemley, *Am. Mineral.* **80**, 222 (1995).

⁷J.B. Parise, K. Leinenweber, D.J. Weidner, K. Tan, and R.B.V. Dreele, *Am. Mineral.* **79**, 193 (1994).

⁸T. Nagai, T. Ito, T. Hattori, and T. Yamanaka, *Phys. Chem. Miner.* **27**, 462 (2000).

⁹J.B. Parise, B. Theroux, R. Li, J.S. Loveday, W.G. Marshall, and S. Klotz, *Phys. Chem. Miner.* **25**, 130 (1998).

¹⁰J.B. Parise, J.S. Loveday, R.J. Nelmes, and H. Kagi, *Phys. Rev. Lett.* **83**, 328 (1999).

¹¹S. Raugei, P.L. Silverstrelli, and M. Parinello, *Phys. Rev. Lett.* **83**, 2222 (1999).

¹²D.M. Sherman, *Am. Mineral.* **76**, 1769 (1991).

¹³J.B. Parise, H. Kagi, J.S. Loveday, R.J. Nelmes, and W.G. Marshall, in *Physics Meets Mineralogy*, edited by H. Aoki (Cambridge University Press, Cambridge, 2000), p. 308.

¹⁴F. Zigan and R. Rothbauer, *Neues Jahrb. Mineral., Monatsh.* **1967**, 137.

¹⁵W.R. Busing and H.A. Levy, *J. Phys. Chem.* **26**, 563 (1957).

¹⁶L. Desgranges, D. Grebille, G. Calvarin, G. Chevrier, N. Floquet, and J. Niepce, *Acta Crystallogr., Sect. B: Struct. Sci.* **49**, 812 (1993).

¹⁷L. Desgranges, G. Calvarin, and G. Chevrier, *Acta Crystallogr., Sect. B: Struct. Sci.* **52**, 82 (1996).

¹⁸T.S. Duffy, J. Shu, H.K. Mao, and R.J. Hemley, *Phys. Chem. Miner.* **22**, 277 (1995).

¹⁹H.K. Mao, J. Xu, and P.M. Bell, *J. Geophys. Res.* **91**, 4673 (1986).

²⁰A.F. Goncharov, V.V. Struzhkin, R.J. Hemley, H.K. Mao, and Z. Liu, in *Science and Technology of High Pressure*, edited by M.H. Manghnani, W.J. Nellis, and M.F. Nicol (University Press, India, 2000), p. 90.

²¹S.-H. Shim and T.S. Duffy, *Am. Mineral.* **87**, 318 (2001).

²²S.S. Mitra, in *Solid State Physics*, edited by F. Seitz and D. Turnbull (Academic, New York, 1962), p. 1.

²³H.D. Lutz, H. Moller, and M. Schmidt, *J. Mol. Struct.* **328**, 121 (1994).

²⁴C. Greaves and M.A. Thomas, *Acta Crystallogr., Sect. B: Struct. Sci.* **42**, 51 (1986).

²⁵M.C. Bernard, R. Cortes, and M. Keddam, *J. Power Sources* **63**, 247 (1996).

²⁶C. Mockenhaupt, T. Zeiske, and H.D. Lutz, *J. Mol. Struct.* **443**, 191 (1998).

²⁷G. Brindley and C.C. Kao, *Phys. Chem. Miner.* **10**, 187 (1984).

- ²⁸D.L. Heinz and R. Jeanloz, *J. Appl. Phys.* **55**, 885 (1984).
- ²⁹C. Murli, S. Sharma, S.K. Kulshreshtha, and S.K. Sikka, *Physica B* **307**, 111 (2001).
- ³⁰R. Lu, A.F. Goncharov, H.K. Mao, and R.J. Hemley, in *Synchrotron Infrared Microspectroscopy: Application to Hydrous Minerals*, edited by G.S.D. Schultze and P.M. Bertsch (Clay Mineral Society, Boulder, CO, 1999), Vol. 9, p. 164.
- ³¹C. Closmann and Q. Williams, *Am. Mineral.* **80**, 201 (1995).
- ³²A.K. Kleppe, A.P. Jephcoat, and N.L. Ross, *Am. Mineral.* **86**, 1275 (2001).
- ³³D.J. Frost and Y. Fei, *J. Geophys. Res.* **103**, 7463 (1998).
- ³⁴H. Yang, C.T. Prewitt, and D.J. Frost, *Am. Mineral.* **82**, 651 (1997).
- ³⁵E. Libowitzky, *Monatsch. Chem.* **130**, 1047 (1999).
- ³⁶P. Dawson, C.D. Hadfield, and G.R. Wilkinson, *J. Phys. Chem. Solids* **34**, 1217 (1973).
- ³⁷S. R. Shieh and T. S. Duffy (unpublished).